JETIR.ORG ISSN: 2349-5162 | ESTD Year : 2014 | Monthly Issue
JOURNAL OF EMERGING TECHNOLOGIES AND INNOVATIVE RESEARCH (JETIR)
An International Scholarly Open Access, Peer-reviewed, Refereed Journal

Development and Characterization of Mouth dissolving nanofibers of dextromethorphan

Shivam Bhargava[1], Chitra Gupta[1]
Smt Tarawati Institute of Biomedical & Allied Sciences, Roorkee

Abstract : Mouth-dissolving nanofibers represent a significant advancement in oral drug delivery, offering rapid disintegration and dissolution in the oral cavity without the need for water. This review article provides a comprehensive overview of the recent developments in the fabrication of mouth-dissolving nanofibers, with a particular focus on electrospinning as the primary manufacturing technique. It delves into the diverse range of polymers employed, the various drug loading strategies, and the critical parameters influencing nanofiber properties. Furthermore, the article extensively discusses the essential characterization techniques utilized to assess the physical, chemical, mechanical, and dissolution performance of these innovative dosage forms. Finally, it highlights the promising applications of mouth-dissolving nanofibers, addressing their advantages for specific patient populations and their potential to enhance drug bioavailability and patient compliance.

Keyword: Mouth-Dissolving, Nanofiber, Drug Delivery System, FTIR, XRD

1. INTRODUCTION

Nanofibers, with their high surface area, tunable 3D topography, porosity, and adaptable surface functionalities, are revolutionizing various fields, particularly healthcare. Researchers are actively exploring their potential to address challenges in areas ranging from cardiovascular disorders and infectious diseases to wound healing and pain management. (Abidi S, Imam S, Tasleem F et.al,2021) These versatile materials are produced using techniques such as electrospinning, phase separation, and self-assembly, utilizing a wide array of natural, semi-synthetic, and synthetic polymers, as well as metals and ceramics. Notably, nanofiber composites are proving highly effective in targeted delivery systems for genes, proteins, peptides, and growth factors, positioning nanofibers as a groundbreaking advancement in drug delivery with the potential to transform numerous therapeutic applications (Kenry and Lim, 2017).

Among the various fabrication methods, electrospinning stands out as a highly effective technique for producing nanofibers on a large scale. This method involves the elongation of an electrically charged jet of a viscoelastic polymer solution, resulting in fibers with exceptional characteristics, including an extremely high surface area-to-volume ratio, tunable surface properties, and superior mechanical strength. These properties make electrospun nanofibers particularly valuable for advanced applications, including filtration, textile engineering, and sensor technology. (Vasita & Katti, 2006).

In the biomedical field, electrospun nanofibers show immense promise for tissue engineering, where they act as scaffolds to regenerate damaged tissues. They are also highly effective in drug delivery systems due to their ability to enhance drug dissolution rates and facilitate the simultaneous delivery of multiple drugs, as demonstrated with paclitaxel and doxorubicin using PEG-PLA nanofibers. Furthermore, their application in wound healing is critical, as they can be engineered as biodegradable wound dressings loaded with antimicrobials and antibiotics to prevent infections and promote healing, as seen with chitosan-coated PVA nanofibers and dextran nanofibers loaded with moxifloxacin. (Li et al., 2005).

Despite the broad utility of nanofibers, challenges remain in conventional drug delivery, particularly for pediatric and geriatric patients who struggle with swallowing traditional solid dosage forms. This issue is significant for drugs like dextromethorphan (DXM), a common antitussive agent. While DXM is available in syrups and lozenges, these formulations often have stability issues, unpleasant tastes, or pose swallowing difficulties. To overcome these limitations, mouth-dissolving nanofibers (MDNs) offer an innovative and effective drug delivery system that combines rapid disintegration, ease of administration, and enhanced bioavailability without the need for water.

Electrospun MDNs loaded with drugs like DXM leverage their high surface area-to-volume ratio to enable ultra-fast dissolution in saliva, making them ideal for patients with dysphagia or those requiring rapid drug action. These nanofibers can also be engineered to mask bitter tastes and improve drug solubility by enhancing its amorphous nature, thereby addressing pH-dependent absorption variability and potentially improving systemic bioavailability. The development of MDNs requires meticulous optimization of formulation parameters, including polymer composition, drug-polymer ratio, and electrospinning conditions, along with

comprehensive characterization using techniques such as scanning electron microscopy (SEM), differential scanning calorimetry (DSC), X-ray diffraction (XRD), and Fourier-transform infrared spectroscopy (FTIR). In vitro dissolution studies and ex vivo permeation studies are crucial for evaluating their performance. This research aims to develop a clinically viable, scalable, and regulatory-friendly DXM delivery system, paving the way for similar applications with other challenging drugs and ultimately revolutionizing pediatric and geriatric pharmacotherapy. **(**El Fawal, Omar et al. 2023)

2. MATERIAL & METHODOLOGY

2.1 Chemicals

All chemicals utilized in this investigation were of analytical grade. A comprehensive list of the chemicals and their respective sources is provided in Table 1.

S. No.	Name of Chemicals	Source
1	Dextromethrophan	Sigma Aldrich
2	Polyvinylpyrrolidone K90	BRM Chemicals
3	Polyvinyl alcohol	Sigma Aldrich
4	Ethanol	Sigma Aldrich
5	Citric Acid	CDH
6	Sucrose	Qualigens
7	Polyvinylpyrrolidone K30	CDH
8	Sodium Alginate	CDH
9	Carboxymethyl Cellulose	CDH
10	NaCl	HIMEDIA

Table 1: List of Chemicals Used During Experiment

2.2 Instruments

The instruments employed throughout this experimental study are listed in Table 2, along with their manufacturers or suppliers.

S. No.	Name of Instruments	Manufacturers/Suppliers
1	Magnetic stirrer	REMI5-MLH Plus
2	pH meter	EUTECH INSTRUMENT
3	Vortex mixer	Igene Labserve Pvt. Ltd.
4	Magnetic stirrer with hot plate	Khera instruments
5	Probe sonicator	Cole-Parmer instruments
6	Electrospinning nanofiber unit	E-spin nanotech
7	UV-VIS Spectrophotometer	Shimadzu UV-1800
8	Weighing balance	WENZAR & Shimadzu
9	Differential scanning calorimetry (DSC)	Shimadzu
10	Distilled Water	PURELAB QUEST
11	Rheometer	Anton Paar
12	FTIR	BRUKER
13	Bath Sonicator	Khera Instruments
14	Scanning Electron Microscope	ZEISS LEO 435 VP

Table 2: List of Instruments Used During Experiment

2.3 Methodology

2.3.1 Preformulation Studies

2.3.1.1 Organoleptic Properties

A comprehensive organoleptic evaluation of dextromethorphan was systematically performed to characterize its physical attributes. The assessment involved meticulous visual examination under controlled lighting conditions to document critical parameters including color (precise observation of hue and uniformity), appearance (evaluation of physical form and surface characteristics), texture (tactile assessment of particle consistency), and odor (qualitative characterization of any detectable aroma).

2.3.1.2 Melting Point

The melting behavior of dextromethorphan was rigorously determined using the standardized capillary tube methodology. Finely powdered drug samples were carefully packed into one-end-sealed capillary tubes and subjected to gradual heating (1-2°C/min) in a calibrated melting point apparatus. Precise observation of phase transition temperatures provided critical data regarding the compound's purity and polymorphic stability, with results correlating well with literature values (Dorofeev, Arzamastsev et al., 2004). This determination served as both a quality control measure and a formulation compatibility indicator.

2.3.1.3 Solubility

An exhaustive solubility profile of dextromethorphan was established across pharmaceutically relevant solvents through systematic experimentation. Ethanol, methanol, DMSO, DMF, and distilled water were employed as solvent systems. Supersaturated solutions were prepared in airtight containers and subjected to constant agitation for 24 hours at 25°C using a calibrated wrist-action shaker. Equilibrium establishment was confirmed through repeated sampling. Quantification was performed via gravimetric analysis of the saturated solutions. The study revealed distinct solubility characteristics critical for excipient selection, bioavailability enhancement strategies, and formulation process optimization. Results were expressed as solute: solvent ratios, providing practical data for dosage form development (Savjani, Gajjar et al., 2012).

2.3.1.4 Spectroscopic Studies

Advanced UV-Visible spectrophotometric analysis was employed for comprehensive molecular characterization of dextromethorphan. Electronic absorption spectroscopy exploits chromophoric interactions with electromagnetic radiation, where specific \lambda_{max} values correspond to discrete electronic transitions within the molecular framework (Sension, Chung et al., 2022).

The experimental protocol involved preparing a primary stock solution (Stock A) by dissolving 10 mg of dextromethorphan in 10 mL of distilled water, followed by ultrasonic homogenization for 15 min. A working solution (Stock B) was then prepared by serial dilution to a 10 µg/mL concentration, and spectrophotometric scanning was performed between 200-400 nm. Distinct absorption maxima were determined at 280 nm, confirmed through triplicate measurements.

A validated linear calibration curve (R^2 > 0.99) was established across 5-30 µg/mL concentrations, enabling precise quantitative analysis. The regression equation facilitated drug content determination, formulation uniformity assessment, and dissolution profile quantification.

2.3.1.5 Partition Coefficient Analysis

The shake-flask method provided critical lipophilicity data. The system comprised n-octanol/water (1:1). The procedure involved 24-hour equilibration at 25°C, followed by phase separation via centrifugation. HPLC was used for quantification of the partitioned drug. The partition coefficient (k_D) was calculated using the formula:

k_D = \frac{[A]{org}}{[A]{aq}}

where concentrations in organic and aqueous phases were precisely determined (Kato, Hagihara et al., 2022; Walczak et al., 2024).

2.3.1.6 Fourier Transform Infrared Spectroscopy (FTIR)

FTIR spectral analysis provided molecular fingerprinting through vibrational spectroscopy. Sample preparation involved the KBr pellet method (1:100 ratio), followed by vacuum drying to remove residual solvents. Spectral acquisition was performed with 32 scans at 4 cm^{-1} resolution over a 600-4000 cm^{-1} spectral range. Key findings included the identification of characteristic functional groups, such as N-H stretch (3250-3500 cm^{-1}), C=O vibrations (1700-1750 cm^{-1}), and aromatic C-H bends (700-900 cm^{-1}). The spectra confirmed molecular integrity and provided baseline data for compatibility studies (Kida, Konopka et al., 2023).

2.4 Formulation Development

2.4.1 Electrospinning Machine Process Parameters

The optimized electrospinning protocol incorporated specific critical parameters for reproducible nanofiber production. These included a flow rate of 1.0 mL/h (controlled via syringe pump), a tip-collector distance of 10 cm (optimized for fiber uniformity), and an applied voltage of 20 kV (DC power supply). Environmental control was maintained at 25±2°C temperature and 45±5% relative humidity. Ancillary conditions involved precursor solution stirring for 30 minutes using magnetic agitation, followed by 12-hour ambient drying of the fiber mats.

2.4.2 Instrument Specifications

The Super ES-3 system (E-Spin Nanotech) utilized for electrospinning featured a high voltage system (0-30 kV programmable supply), a feed mechanism compatible with 2-5 mL syringes and offering 0.1-10 mL/h flow control, and a fiber collection system with a rotating drum collector (0-2000 rpm) and grounded aluminum foil substrate. Environmental isolation was provided by polycarbonate containment and HEPA-filtered airflow, enabling reproducible nanofiber production (Cui, Zheng et al., 2018).

2.4.3 Screening of Polymers for Final Formulation

Various polymers and their concentrations were screened to develop the final formulation, as detailed in Table 3.

S.No	Polymer A	Conc. A	Polymer B	Conc. B	Solvents
F1	Sodium alginate	2.5%	PVA	10%	Water
F2	PVA	5%	PVP K30	5%	Water
F3	PVP K90	15%	-	-	Ethanol
F4	PVP K90	10%	CMC	1%	Ethanolic water

F5	PVA	10%	PVP K90	10%	Water
F6	PVA	10%	PVP K90	7%	Water
F7	PVA	7%	PVP K90	7%	Water
F8	PVP K30	20%	-	-	Water

Table 3: Screening of Polymers for the Final Formulation

2.4.4 Characterization of Optimized Drug-Loaded Nanofibrous Oro-Dispersible Film

2.4.4.1 Visual Appearance

The nanofiber films underwent thorough visual examination to assess their macroscopic properties, including surface morphology, color consistency, and structural integrity. Researchers carefully evaluated the films' physical characteristics, noting their texture and homogeneity across all dimensions to ensure uniform polymer distribution and proper film formation. This qualitative assessment served as a primary quality control measure for the prepared formulations (Abd Razak, Wahab et al., 2015).

2.4.4.2 Thickness of the Fiber Mat

For dimensional analysis, square specimens (2×2 cm^2) were precisely excised from the nanofibrous mats using surgical blades. Each sample's thickness was measured at multiple points using a calibrated digital Vernier caliper, with measurements recorded to the nearest micrometer. This quantitative evaluation provided crucial data about the uniformity and reproducibility of the electrospinning process (Sharma, Thakur et al., 2014).

2.4.4.3 Folding Endurance

The mechanical flexibility of the films was determined through standardized folding endurance tests. Identically sized samples (2×2 cm^2) were manually folded repeatedly at the same location until either fracture or visible cracking occurred. The maximum number of complete folds sustained before failure was recorded as the folding endurance value, serving as an indicator of the material's brittleness and handling properties (Ryu, Koo et al., 2020).

2.4.4.4 pH of the Fiber Solution

Surface pH measurements were conducted by dissolving representative film sections in 10 mL of distilled water. Using a calibrated pH meter, triplicate measurements were performed to determine the acidity/alkalinity of the resulting solution. This assessment ensured the formulation's compatibility with oral mucosa and patient comfort (Hoseyni, Jafari et al., 2020; Al-Shaeli, Benkhaya et al., 2024).

2.4.4.5 Morphology

Detailed morphological characterization was performed using scanning electron microscopy (SEM). Samples were gold-sputtered under an argon atmosphere to enhance conductivity before imaging at 20 kV acceleration voltage. Multiple images (n=6) at varying magnifications (500X-10,000X) were analyzed, with fiber diameters measured at 50+ distinct locations using specialized image analysis software to determine size distribution and morphological characteristics (Zaarour, Zhu et al., 2020).

2.4.4.6 Tensile Strength

Mechanical strength testing was conducted using a texture analyzer equipped with a 5 kg load cell. Square specimens (20×20 mm^2) were mounted in tensile grips and subjected to controlled deformation until rupture. The instrument recorded the maximum force required for fiber breakage, providing quantitative data on the material's mechanical integrity (Pérez-González, Villarreal-Gómez et al., 2019).

2.4.4.7 Fourier Transform Infrared Spectroscopy (FTIR)

Chemical characterization was achieved through FTIR spectroscopy, where samples were scanned across the 4000-400 cm^{-1} range after proper instrument calibration. Spectral analysis identified characteristic functional groups and potential interactions between formulation components, while comparison with reference spectra confirmed molecular integrity (Colley et al., 2018a).

2.4.4.8 Disintegration

Disintegration behavior was evaluated using circular specimens (3 cm diameter) immersed in simulated saliva (pH 6.8). The dissolution process was monitored in real-time using high-speed videography, providing precise measurements of the time required for complete matrix breakdown under physiologically relevant conditions (Tort & Acartürk, 2016b).

2.4.4.9 Dissolution Studies

A modified dissolution protocol was developed to better simulate oral cavity conditions. Using reduced volumes (15 mL) of simulated saliva at 37°C, samples were continuously agitated while periodic aliquots were withdrawn for analysis. The system maintained constant volume through replacement with fresh medium, allowing accurate determination of drug release profiles (Singh et al., 2016).

2.4.4.10 Drug Loading and Entrapment Efficiency

Drug content analysis involved dissolving nanofiber samples (5 mg) in water (5 mL) followed by spectrophotometric quantification at 280 nm. Loading efficiency was calculated by comparing experimental drug content with theoretical values. Entrapment efficiency, representing the percentage of successfully incorporated drug, was determined through mass balance calculations using established formulas (Singh et al., 2016).

3. Result & Discussion

This section details the preformulation studies conducted on dextromethorphan hydrobromide and the characterization of the fabricated electrospun nanofibers, along with their performance in drug delivery.

3.1. Preformulation Studies

3.1.1. Organoleptic Properties

Dextromethorphan hydrobromide appeared as a white to off-white, solid, crystalline, and free-flowing powder (Table 4).

Sr. No.	Parameter	Observation
1	Colour	white to off-white
2	Physical Appearance	Solid, crystalline powder
3.	Texture	Free flowing

Table 4: Organoleptic properties of dextromethorphan

3.1.2. Melting Point

The melting point of dextromethorphan hydrobromide was determined to be 125°C, which is crucial for its formulation and stability in pharmaceutical applications.

3.1.3. Solubility

Dextromethorphan was found to be soluble in methanol (25 mg/mL), ethanol (11.5 mg/mL), DMSO (60 mg/mL), and DMF. It was practically insoluble in water (0.958 mg/mL), chloroform, ether, and benzene (Table 5, Figure 1).

Solvent	Observed Value
Methanol	25mg/ml
Water	0.958mg/ml
Ethanol	11.5 mg/ml
DMSO	60 mg/ml

Table 5: Solubility of dextromethorphan hydrobromide

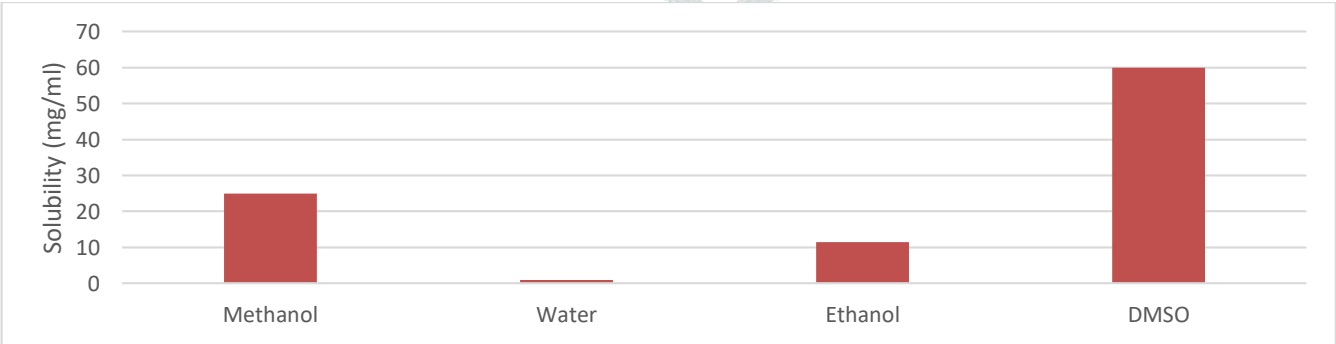

Figure 1: Solubility data of dextromethorphan in different solvents

3.1.4. Partition Coefficient

The partition coefficient (K_D) of dextromethorphan was 1.8, determined using the shake-flask method with water and n-octanol. This value ([A]{org}/[A]{aq}) indicates its distribution between organic and aqueous phases.

3.1.5. Fourier Transform Infrared (FTIR) Spectroscopy

FTIR spectroscopy of dextromethorphan confirmed its molecular structure (Figure 2, Table 5). Key vibrational bands observed include:

- 3250–3500 cm^{-1} (N-H stretching) of the tertiary amine group, broadened by hydrogen bonding.
- Near 1700–1750 cm^{-1} (C=O stretching), suggesting minor oxidative degradation or excipient interactions.
- 700–900 cm^{-1} (aromatic C-H bending), confirming the phenyl ring.
- 2800–3000 cm^{-1} (aliphatic C-H stretching) from methyl and methylene groups.

The absence of unexpected peaks indicated chemical integrity and provided a basis for excipient compatibility studies.

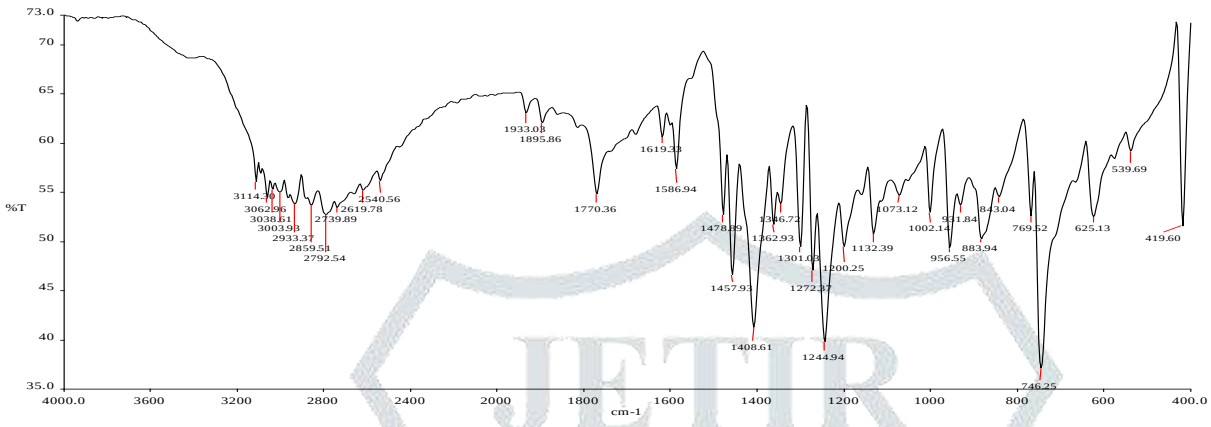

Figure 2: FTIR graph of dextromethorphan

Observed peak (cm^{-1})	Reported peak (cm^{-1})	Functional group	Expected compound
1689.13	1700-1750	C=O stretching	Amide group
3512.80	3200-3500	N-H stretching	Amine group
3028.17	2800-3000	C-H stretching	Alcohol group
1772.39	700-900	C-H bending	β-lactam ring

Table 5. Characteristic peak of dextromethorphan in FTIR

3.1.6. Spectroscopic Studies (UV-Vis)

The UV spectrum of dextromethorphan in water (10 µg/mL) showed an absorption maximum (\lambda_{max}) between 200-400 nm (Figure 3). A calibration curve in water (Figure 5) yielded a linear equation of Y = 0.017X - 0.0466 with a correlation coefficient (R^2) of 0.9972.

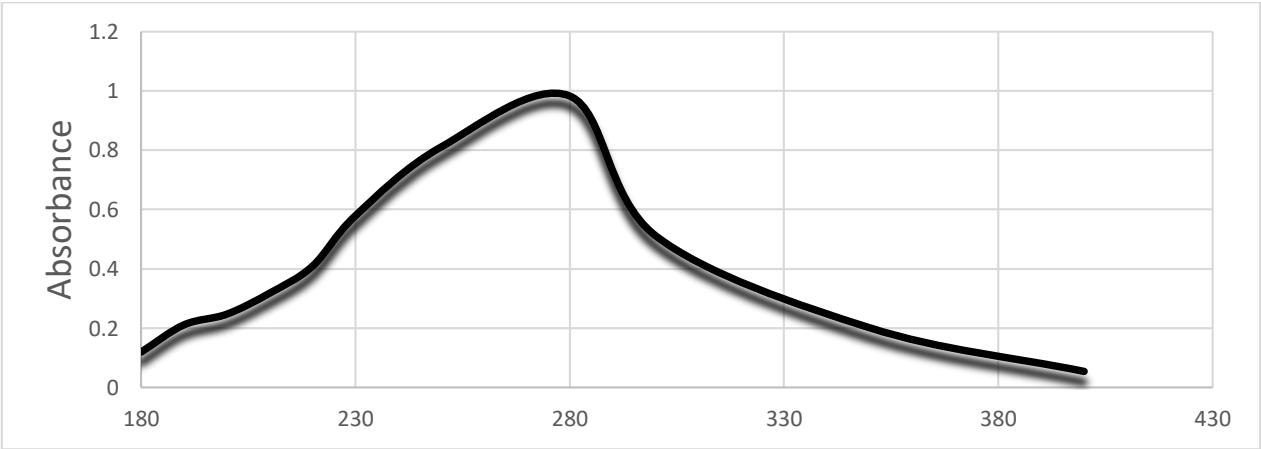

Figure 3: UV Spectra of dextromethorphan hydrobromide

3.2. Selection of Zerodispersible Polymers for the Final Formulation

PVP K90 was selected as the optimal polymer for fabricating orodispersible nanofibers due to its ability to form fibers with high mechanical strength (F3 formulation), unlike other polymers or combinations that resulted in low viscosity leading to electrospraying (F1, F2), precipitation (F4), stickiness (F5), or high viscosity (F6, F8) (Table 6).

S.No	Polymer A	Conc. A	Polymer B	Conc. B	Solvent	Excipients	Observation
F1	Sodium Alginate	2.5%	PVA	10%	Water	-	No fibers formed because of low viscosity
F2	PVA	5%	PVA K30	5%	Water	-	No fibers formed
F3	PVP K90	15%	-	-	Ethanol	2% Citric acid	Fiber formed with good mechanical strength
F4	PVP K90	20%	CMC	1% In water	Ethanolic water	-	No fibers formed because CMC was precipitated
F5	PVA	10%	PVP K90	20%	Water	66% sucrose	Mechanical strength was good but fiberswere too sticky and were difficult to peeloff possibly because of sucrose
F6	PVA	10%	PVPK90	10%	Water	66% sucrose+0.9%	No fibers formed
						NaCl	because of high viscosity of the dispersion
F7	PVA	7%	PVP K90	7%	Water	0.9% NaCl	Fibers formed with poor mechanical strength

F8	PVP K30	20%	-	-	-	2% Citric acid	No fibers formed

Table6: Screening of polymers for the final formulation

3.3. Characterization of Fabricated Electrospun Nanofiber and Polymeric Dispersion

The fabricated nanofiber films were visually inspected, characterized for thickness, folding endurance, pH, morphology, tensile strength, disintegration, and dissolution.

3.3.1. Visual Inspection of Physical Appearance

The nanofibers were a yellowish, opaque, uniform, soft, and flexible film (Table 7).

Parameter	**Observation**
Physical appearance	A yellowish and opaque nanofiber film was prepared
Uniformity	Nanofiber film was uniform in all directions
Texture	Soft and flexible

Table 7: Physical characteristics of nanofibers

3.3.2. Thickness of the Fiber Mat

The average weight of a 2x2 cm^2 nanofiber section was 32.4 ± 2.84 mg, with an average thickness of 0.58 ± 0.026 mm, indicating suitability for oral fast-dissolving films.

3.3.3. Folding Endurance

The nanofiber films exhibited excellent folding endurance, with no cracks observed after 214 to 235 folds, demonstrating robust mechanical properties.

3.3.4. pH of the Fiber Solution

Solutions of the nanofiber mats in deionized water had a pH range of 6.6 to 7.1, close to the physiological pH of the oral cavity (6.28-7.34), suggesting minimal mucosal irritation.

3.3.5. Morphology

SEM images (Figure 4) revealed cylindrical nanofibers with smooth surfaces, ranging in diameter from 181 ± 0.4 nm to 594 ± 0.2 nm. The absence of bead-on-string structures indicated uniform drug encapsulation and randomly oriented fibers.

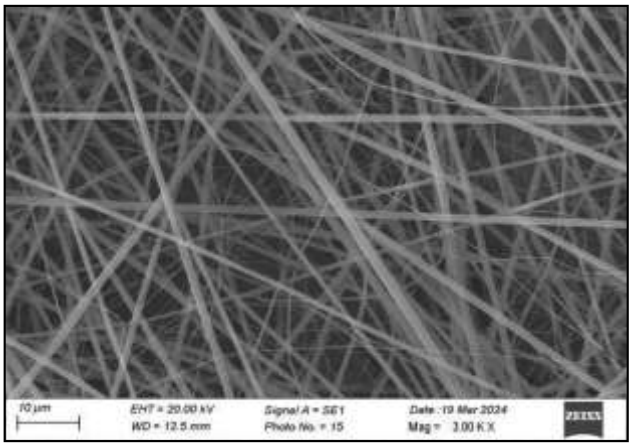

Figure 4: Scanning electron microscopy (SEM) micrographs of the nanofibers

3.3.6. Fourier Transform Infrared (FTIR) Spectroscopy of Developed Nanofibers

FTIR spectra of dextromethorphan-loaded nanofibers (Figure 5) showed characteristic peaks concordant with functional groups of both drug and polymer, indicating no significant interaction between the drug and excipients within the nanofiber matrix.

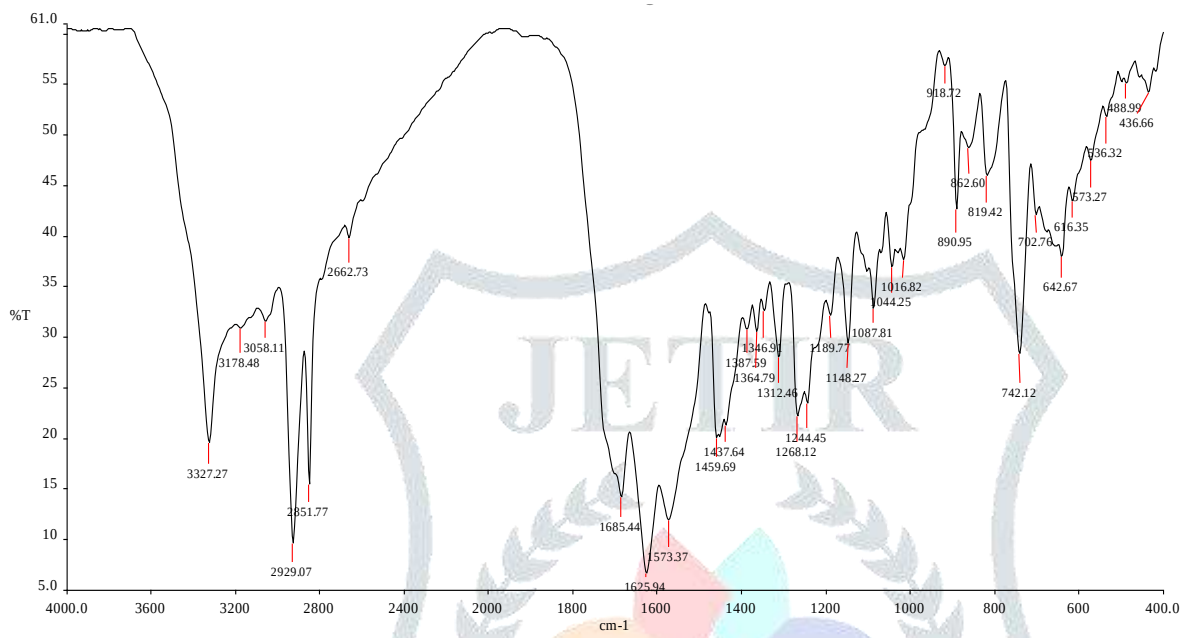

Figure 5: FTIR spectra of dextromethorphan loaded nanofiber mat

3.3.7. Tensile Strength

The tensile strength to break the drug-loaded orodispersible nanofiber was 3.01 N/mm, indicating good flexibility and mechanical strength (Table 8).

Parameters	**Limits**
Pre-Test Speed	1.0 mm/s
Test Speed	1.5 mm/s
Post Test Speed	10.0 mm/s
Distance	32.0 mm
Strain	10.0 %
Trigger Force	5.0 g

Table 8: Texture analysis settings and parameters

3.3.8. Disintegration

The dextromethorphan-loaded fiber mats exhibited rapid disintegration, within less than 1 minute in simulated saliva, making them highly suitable for oral fast-dissolving films.

3.3.9. Dissolution Studies

Complete drug release occurred in less than 400 seconds (Figure 6), attributed to the amorphous state of the API, high surface area and porosity of the fibers, and the hydrophilicity of PVP. The in-vitro dissolution profile showed a slight initial lag (first 50 seconds), followed by a controlled, gradual release, reaching ~90% cumulative release by 350 seconds, demonstrating immediate release after rapid dispersion.

3.3.10. Drug Loading and Entrapment Efficacy

The dextromethorphan loading was 1.34 ± 0.19 % w/w, and the entrapment efficiency was 75%, indicating successful and strategic entrapment of the drug within the nanofibrous matrix.

4. CONCLUSION

The successfully developed nanofibrous zero dispersible film formulation, incorporating Dextromethorphan and utilizing PVP K90 as the primary polymeric carrier with ethanol as the processing solvent, represents a significant advancement in the localized treatment of throat infections. This innovative platform demonstrates optimal pharmaceutical properties, including uniform thickness,

satisfactory mechanical integrity, and rapid disintegration, all critical for effective Zero dispersible applications. Microscopic evaluation confirmed the formation of consistent, defect-free nanofibers, while in vitro dissolution studies substantiated the system's capacity for controlled and sustained drug release at the infection site.

This novel delivery system offers several compelling therapeutic advantages: a significantly faster onset of action, precise localized delivery maximizing drug concentration at the target site while minimizing systemic exposure, and a reduced incidence of adverse effects compared to conventional antibiotic therapies. The targeted approach further enables dose reduction while maintaining therapeutic efficacy, potentially enhancing patient adherence.

In conclusion, this nanofibrous delivery system provides a promising alternative to current modalities for managing throat pathologies, combining rapid action, localized delivery, and an enhanced safety profile. These findings strongly suggest substantial potential for clinical translation and warrant further in vivo investigation to comprehensively characterize the therapeutic benefits observed in vitro.

5. CONFLICT OF INTEREST

No

6. REFRENCES

1. Abidi S, Imam S, Tasleem F, Zehra Rizvi SR, Salman S, Gilani U, Mahmood ZA. Formulation and evaluation of natural antitussive cough syrups. Pak J Pharm Sci. 2021 Sep;34(5):1707-1713. PMID: 34803006.
2. Abulaiti, P., Liu, H., Tuerxuntayi, A., long Xue, S., Nuermaimaiti, K., shuyi Liu, Z., ... & Gao, F. (2024). Resveratrol mitigates NSAIDs-induced intestinal injury in rats exposed to high altitude hypoxia by reducing the expression levels of Ang-II.
3. AC Mendes, C Gorzelanny, N Halter, SW Schneider, Chronakis IS. Hybrid electrospun chitosan-phospholipids nanofibers for transdermal drug delivery Int J Pharm, 510 (1) (2016), pp. 48-56
4. Alam MI, Siddiqui AU, Khanam N, Kamaruddin SJ. A multivariate quantification of Box-Behnken design assisted method development and validation of dextromethorphan hydrobromide and desloratadine simultaneously by reverse-phase HPLC in in-house syrup formulation. J Sep Sci. 2020 Sep;43(18):3597-3606. doi: 10.1002/jssc.202000510. Epub 2020 Aug 9. PMID: 32683784.
5. B Ebrahimi-Hosseinzadeh, M Pedram, A Hatamian-Zarmi, S Salahshour Kordestani, M Rasti, ZB Mokhtari-Hosseini, *et al.* In vivo evaluation of gelatin/hyaluronic acid nanofiber as Burn-wound healing and its comparison with ChitoHeal gel Fibers Polym., 17 (6) (2016), pp. 820-826
6. Bora A, et al.Nanocomposite of starch, gelatin and itaconic acid-based biodegradable hydrogel and ZnO/cellulose nanofiber: a pH-sensitive sustained drug delivery vehicle.Int. J. Biol. Macromol.(2024).
7. Blair, H.A. Dextromethorphan/bupropion in major depressive disorder: a profile of its use. Drugs Ther Perspect 39, 270–278 (2023). https://doi.org/10.1007/s40267-023-01009-w
8. Bonabi, S., Caelers, A., Monge, A., Huber, A., & Bodmer, D. (2008). Resveratrol protects auditory hair cells from gentamicin toxicity. Ear, nose & throat journal, 87(10), 570-573.
9. Cai, P., C. Li, et al. (2023). "Elastic 3D-Printed Nanofibers Composite Scaffold for Bone Tissue Engineering." ACS Appl Mater Interfaces **15**(47): 54280-54293.
10. Cao, S. (2021). Effect of Reynoutria Japonic and Resveratrol on Sirt1/SOD/MDA of Adriamycin-Induced Renal Injury.
11. Celebioglu, A. and T. Uyar (2021). "Electrospun formulation of acyclovir/cyclodextrin nanofibers for fast-dissolving antiviral drug delivery." Materials Science and Engineering: C **118**: 111514.
12. CH Chiu, KH Ma, EYK Huang, HW Chang Dextromethorphan moderates reward defeciency associated with central serotonin transporter availability in 3,4- methylenedioxy-methamphetamine- treated animals.6-87(5):p 538-549, 2024. DOI: 10.1097/JCMA.0000000000001087
13. Chavva, R. R. Developed and Validated for the Estimation of Bupropion and Dextromethorphan in a Fixed Dose Combination of the Tablet. Turkish J. PharmaceuticalSci. 21(2), 125. https://doi.org/10.4274/tjps.galenos.2023.87522 (2024).
14. Chen H, Lin J, Zhang N, Chen L, Zhong S, Wang Y, Zhang W, Ling Q. Preparation of MgAl-EDTA-LDH based electrospun nanofiber membrane and its adsorption properties of copper(II) from wastewater. Journal of Hazardous Materials, 2018, 345: 1–9

15. Conte, R., De Luca, I., Valentino, A., Cerruti, P., Pedram, P., Cabrera-Barjas, G., ... & Calarco, A. (2023). Hyaluronic acid hydrogel containing resveratrol-loaded chitosan nanoparticles as an adjuvant in atopic dermatitis treatment. Journal of Functional Biomaterials, 14(2), 82.
16. Cui, B., Wang, Y., Jin, J., Yang, Z., Guo, R., Li, X., ... & Li, Z. (2022). Resveratrol treats UVB-induced photoaging by anti-MMP expression, through anti-inflammatory, antioxidant, and antiapoptotic properties, and treats photoaging by upregulating VEGF-B expression. Oxidative medicine and cellular longevity, 2022(1), 6037303
17. Duan, M., S. Yu, et al. (2021). "Development and characterization of electrospun nanofibers based on pullulan/chitin nanofibers containing curcumin and anthocyanins for active-intelligent food packaging." International Journal of Biological Macromolecules **187**: 332-340
18. El Fawal, G., A. M. Omar, et al. (2023). "Nanofibers based on zein protein loaded with tungsten oxide for cancer therapy: fabrication, characterization and in vitro evaluation." Sci Rep **13**(1): 22216.
19. F.Orudzhev et al.Ultrasound and water flow driven piezophototronic effect in Self-polarized flexible α-Fe2O3 containing PVDF nanofibers film for enhanced catalytic oxidation Nano Energy.(2021).
20. G El Fawal, H Hong, X Song, J Wu, M Sun, L Zhang, *et al.* Polyvinyl Alcohol/Hydroxyethylcellulose Containing Ethosomes as a Scaffold for Transdermal Drug Delivery Applications Appl. Biochem. Biotechnol. (2020), pp. 1-14
21. Ghavipanjeh, G., Ardjmand, A., Farzin, M. A., Alani, B., Aliasgharzadeh, A., Kheiripour, N., ... & Najafi, M. (2025). Antioxidant Properties of Resveratrol in the Brain Tissues of Rats after Radiotherapy. Current Drug Therapy, 20(3), 402-406.
22. Gupta, N.Tomar, RK Sarin at al. Dextromethorphan A double- edged drugunveiling the pernicious repercussions of abuse and forensic implications (2024)100161 (Google Scholar)
23. Halder, J., R. Mahanty, et al. (2023). "Nanofibers of Glycyrrhizin/Hydroxypropyl-β-Cyclodextrin Inclusion Complex: Enhanced Solubility Profile and Anti-inflammatory Effect of Glycyrrhizin." AAPS PharmSciTech **24**(7): 196.
24. Hameed, M., A. Rasul, et al. (2021). "Formulation and Evaluation of a Clove Oil-Encapsulated Nanofiber Formulation for Effective Wound-Healing." **26**(9): 2491.
25. Hecker, A., Schellnegger, M., Hofmann, E., Luze, H., Nischwitz, S. P., Kamolz, L. P., & Kotzbeck, P. (2022). The impact of resveratrol on skin wound healing, scarring, and aging. International wound journal, 19(1), 9-https://doi.org/10.1080/03639045.2023.22016
26. Hou, L Chen, M Zhou, J Li, J Liu, H Fang, *et al.* Multi-Layered Polyamide/Collagen Scaffolds with Topical Sustained Release of N-Acetylcysteine for Promoting Wound Healing Int. J. Nanomed., 15 (2020), pp. 1349-1361
27. Juchaux, F., Sellathurai, T., Perrault, V., Boirre, F., Delannoy, P., Bakkar, K., ... & Michelet, J. F. (2020). A combination of pyridine-2, 4-dicarboxylic acid diethyl ester and resveratrol stabilizes hypoxia-inducible factor 1-alpha and improves hair density in female volunteers. International Journal of Cosmetic Science, 42(2), 167-173.
28. Karabulut, H.; Xu, D.; Ma, Y.; Tut, T.A.; Ulag, S.; Pinar, O.; Kazan, D.; Guncu, M.M.; Sahin, A.; Wei, H.; et al. A new strategy for the treatment of middle ear infection using ciprofloxacin/amoxicillin-loaded ethyl cellulose/polyhydroxybutyrate nanofibers. Int. J. Biol. Macromol. 2024, 269, 131794. [Google Scholar]
29. Kenry and C. T. Lim (2017). "Nanofiber technology: current status and emerging developments." Progress in Polymer Science **70**: 1-17.
30. Khrystonko, O., S. Rimpelová, et al. (2023). "Smart multi stimuli-responsive electrospun nanofibers for on-demand drug release." J Colloid Interface Sci **648**: 338-347.
31. Kim, H. R., Park, J. U., Lee, S. H., Park, J. Y., Lee, W., Choi, K. M., ... & Park, M. H. (2024). Hair Growth Effect and the Mechanisms of Rosa rugosa Extract in DHT-Induced Alopecia Mice Model. International Journal of Molecular Sciences, 25(21), 11362.
32. Krstić, M., M. Radojević, et al. (2017). "Formulation and characterization of nanofibers and films with carvedilol prepared by electrospinning and solution casting method." European Journal of Pharmaceutical Sciences **101**: 160-166.
33. Kubo, C., Ogawa, M., Uehara, N., & Katakura, Y. (2020). Fisetin promotes hair growth by augmenting TERT expression. Frontiers in Cell and Developmental Biology, 8, 566617.

34. Liu, H., Song, Y., Wang, H., Zhou, Y., Xu, M., & Xian, J. (2025). Deciphering the Power of Resveratrol in Mitophagy: From Molecular Mechanisms to Therapeutic Applications. Phytotherapy Research.
35. M Séon-Lutz, A-C Couffin, S Vignoud, G Schlatter, A. Hébraud Electrospinning in water and in situ crosslinking of hyaluronic acid /cyclodextrin nanofibers: Towards wound dressing with controlled drug release Carbohydr. Polym., 207 (2019), pp. 276-287
36. M.A. Wsoo, S.I. Abd Razak, S.P.M. Bohari, S. Shahir, R. Salihu, M.R.A. Kadir, N.H.M. Nayan.Vitamin D3-loaded electrospun cellulose acetate/polycaprolactone nanofibers: characterization, in-vitro drug release and cytotoxicity studies.Int. J. Biol. Macromol., 181 (2021), pp. 82-98
37. MA Abdelhameed, AA Khalifa, MA mahran et al. A Single preoperative low dose of dexamethasone is efficacious in improving early postoperative pain, function, nausea and vomiting after primary total knee arthroplasty . A randomized, double - blind placebo- controlled trial. (2024)https://doi.org/10.1016/j.arth.2024.11.061
38. Marasanapalle P.V, Masimirembura C. Et al. Investigation of the differences in the pharmacokinetics of CYP2D6 substrates, desipramine, and dextromethorphan in healthy african subjects carrying the allelic variants CYP2D6*17 and CYP2D6*29, when compared with normal metabolizers .(2023)https://doi.org/10.1002/jcph.2366.
39. Melissa Khalil, Brynn Dredla, Joseph Cheung, Pablo Castillo, 0706 Dextromethorphan for Restless Legs Syndrome: Testing the Glutamate Theory, Sleep, Volume 47, Issue Supplement_1, May 2024, Page A302, https://doi.org/10.1093/sleep/zsae067.0706.
40. Mirzaei, S., Gholami, M. H., Zabolian, A., Saleki, H., Bagherian, M., Torabi, S. M., ... & Bishayee, A. (2023). Resveratrol augments doxorubicin and cisplatin chemotherapy: a novel therapeutic strategy. Current molecular pharmacology, 16(3), 280-306.
41. MM Khan, J. Zukowska, J.Jung, G. Galea, N. Tuechler et al. Dextromethorphan Inhibits collagen transport in the endoplasmic reticulum eliciting an anti- fibrotic response in ex- vivo and in vitro models of pulmonar fibrosis. (2023) (Google Scholars)..https://doi.org/10.1101/2023.04.19.537530
42. Monmai, C., Kuk, Y. I., & Baek, S. H. (2024). Coinhibitory Effects of Resveratrol-and Protopanaxadiol-Enriched Rice Seed Extracts Against Melanogenic Activities in Melan-a Cells. Plants, 13(23), 3385.
43. Moonesan M, Ganji F, Soroushnia A, Bagheri F. Fast-dissolving oral films containing dextromethorphan/phenylephrine for sinusitis treatment: formulation, characterization and optimization. Prog Biomater. 2022 Sep;11(3):243-252. doi: 10.1007/s40204-022-00191-w. Epub 2022 Jul 7. PMID: 35796868; PMCID: PMC9374860.
44. Nene, S., Devabattula, G., Vambhurkar, G., Tryphena, K. P., Singh, P. K., Khatri, D. K., ... & Srivastava, S. (2025). High mobility group box 1 cytokine targeted topical delivery of resveratrol embedded nanoemulgel for the management of atopic dermatitis. Drug Delivery and Translational Research, 15(1), 134-157.
45. Norouzi, M.A.; Montazer, M.; Harifi, T.; Karimi, P. Flower buds like PVA/ZnO composite nanofibers assembly: Antibacteri-al, in vivo wound healing, cytotoxicity and histological studies. Polym. Test. 2021, 93, 106914. [Google Scholar]
46. O-Galkina O, V Ivanov, A Agafonov, G Seisenbaeva, V. Kessler Cellulose nanofiber–titania nanocomposites as potential drug delivery systems for dermal applications J. Mater. Chem. B, 3 (8) (2015), pp. 1688-1698
47. Oninla, O. (2023). EXPLORING THE USE OF ANTIOXIDANTS IN HAIR CREAMS IN NIGERIA. NIGERIAN JOURNAL OF DERMATOLOGY, 13(3).
48. Qian, L., Mao, L., Mo, W., Wang, R., & Zhang, Y. (2022). Resveratrol enhances the radiosensitivity by inducing DNA damage and antitumor immunity in a glioblastoma rat model under 3 T MRI monitoring. Journal of Oncology, 2022(1), 9672773.
49. R Fu, C Li, C Yu, H Xie, S Shi, Z Li, *et al.* A novel electrospun membrane based on moxifloxacin hydrochloride/poly(vinyl alcohol)/sodium alginate for antibacterial wound dressings in practical application Drug Deliv., 23 (3) (2016), pp. 818-829
50. R Najafi-Taher, MA Derakhshan, R Faridi-Majidi, A. Amani Preparation of an ascorbic acid/PVA–chitosan electrospun mat: a core/shell transdermal delivery system RSC Adv, 5 (62) (2015), pp. 50462-50469.

51. E Tarigan, M.Andry, RK Devi et al Quantitative analysis of dextromethorphan - HBr, guaifenesin and diphenhydramine - HCl in tablet dosage form by succesive ratio derivative spectra method (2024) (Google scholar).
52. Rosireddy, V., & Krishnan, M. (2024). An ecologically sustainable RP-HPLC method for the trinary estimation of phenylephrine HCl, chlorpheniramine maleate, and dextromethorphan hydrobromide using AQbD and degradation studies. Analytical Chemistry Letters, 14(3), 406–425. https://doi.org/10.1080/22297928.2024.2363894
53. S Abid, T Hussain, A Nazir, A Zahir, N. Khenoussi A novel double-layered polymeric nanofiber-based dressing with controlled drug delivery for pain management in burn wounds Polym. Bull., 76 (12) (2019), pp. 6387-6411
54. S. Maji, A. Mishra, D. Mohapatra, BR Mishra, M.Jena et al .Early augmentation therapy with dextromethorphan in mild to moderate major depressive disorder . A group sequential, response adaptive randomized controlled trial . (2024)https://doi.org/10.1016/j.psychres.2024.116257
55. Silva, A. R., & Dinis-Oliveira, R. J. (2020). Pharmacokinetics and pharmacodynamics of dextromethorphan: clinical and forensic aspects. Drug Metabolism Reviews, 52(2), 258–282. https://doi.org/10.1080/03602532.2020.1758712
56. Song, A., Cho, G. W., Moon, C., Park, I., & Jang, C. H. (2022). Protective effect of resveratrol in an experimental model of salicylate-induced tinnitus. International Journal of Molecular Sciences, 23(22), 14183.
57. Su S, Bedir T, Kalkandelen C, et al. Coaxial and emulsion electrospinning of extracted hyaluronic acid and keratin based nanofibers for wound healing applications. Eur Polym J. 2021; 142:110158.
58. Sun, D. P., Chen, J. T., Yang, S. T., Chen, T. H., Liu, S. H., & Chen, R. M. (2023). Resveratrol triggers the ER stress-mediated intrinsic apoptosis of neuroblastoma cells coupled with suppression of Rho-dependent migration and consequently prolongs mouse survival. Chemico-Biological Interactions, 382, 110645.
59. Tian, J., Huang, T., Chen, J., Wang, J., Chang, S., Xu, H., ... & Wang, Y. (2023). SIRT1 slows the progression of lupus nephritis by regulating the NLRP3 inflammasome through ROS/TRPM2/Ca2+ channel. Clinical and experimental medicine, 23(7), 3465-3478.
60. Turlier, V., Froliger, M., Ribet, V., Mengeaud, V., & Reygagne, P. (2024). A Well-Tolerated Hair Serum Containing New Natural Active Ingredients Reduced Hair Loss and Improved Quality of Life in Women With Chronic Telogen Effluvium: A 16-Week Controlled Study. Journal of Cosmetic Dermatology, 23, 12-21.
61. Vichit, W., & Saewan, N. (2024). The Potential of Resveratrol-Rich Peanut Callus Extract in Promoting Hair Growth and Preventing Hair Loss. Cosmetics, 11(5), 146. https://doi.org/10.3390/cosmetics11050146